Progress In Electromagnetics Research M, Vol. 27, 83–95, 2012

A FAST VOLUME-SURFACE INTEGRAL EQUATION SOLVER FOR SCATTERING FROM HIGH-CONTRAST MATERIALS

Xiaoqiao Deng*, Changqing Gu, Bingzheng Xu, and Zhuo Li

College of Electronic and Information Engineering, Nanjing University of Aeronautics and Astronautics, Nanjing 210016, China

Abstract—This paper presents a generalized volume-surface integral equation (GVSIE) to solve electromagnetic (EM) scattering of high contrast inhomogeneous materials. Then the method of moments (MoM) is employed to solve the GVSIE. The GVSIE technique where the domain is represented by a corresponding uniform background medium coupled with a variation, together representing the overall inhomogeneity, is solve by the method of moments (MoM) using Schaubert-Wilton-Glisson (SWG) and Rao-Wilton-Glisson (RWG) basis functions. The adaptive cross approximation (ACA) algorithm combined with the equivalent dipole-moment (EDM) method are extended to reduce memory and CPU time. A highly effective preconditioning strategy is presented to solve the system of equations without any increase in the computational complexity. Experiments on several problems representative of scattering simulations are given to illustrate the potential of the above proposed techniques for solving EM scattering involving high contrast applications.

1. INTRODUCTION

High contrast inhomogeneous materials can be found in many useful applications. Numerical studies of electromagnetic scattering from high contrast inhomogeneous materials are very important. Perhaps most widely used is the method of moments (MoM). The approach is always based on solving volume integral equations (VIE) for inhomogeneous medium [1] or surface integral equation (SIE) formulations for homogeneous medium [2] of a physical problem. It

Received 29 September 2012, Accepted 14 November 2012, Scheduled 15 November 2012
* Corresponding author: Xiaoqiao Deng (xiaoqiaodeng@gmail.com).

is well known that burdened with the discretization of the object and the surrounding space, the traditional VIE formulations require many unknowns leading to computationally intractable problems. The SIE formulations are often preferred for homogeneous dielectric objects. Integral equation methods based on the Poggio, Miller, Chang, Harrington, Wu, Tsai (PMCHWT) formulations [3–5] are quite flexible in modeling high contrast materials. However, the SIE is still applicable to piecewise homogeneous media. Therefore, a generalized volume-surface integral equations (GVSIE) [6] method is applied to more effectively analyze the electromagnetic (EM) scattering of high contrast inhomogeneous medium in the paper. The method involves a novel factorization of material parameters that alleviates the computational burden associated with typical VIE implementations. In the method, VIE is only used over regions where the material is actually varying, while PMCHWT is employed elsewhere along the boundaries of the equivalent homogeneous background regions. Since the VIE is only used to account for material perturbations, there is a significant alleviation in the discretization rate involving high contrast materials. This method can greatly reduce the number of unknowns, and then reduce the waste of memory and save a great amount of time.

The MoM with Galerkin testing using Schaubert-Wilton-Glisson (SWG) [1] and Rao-Wilton-Glisson (RWG) [2] basis functions is applied to solve the GVSIE. And then the EDM method [7, 8] is extended to accelerate the impedance matrix filling. However, for large scale EM problems, the cost to solve this dense matrix equation produced by EDM/MoM is very expensive and formidable. In order to deal with large objects, a number of successful techniques have been extensively used to reduce memory [9–12]. The adaptive cross approximation (ACA) algorithm [13] which is purely algebraic in nature and relatively easy to implement has been widely applied. The ACA algorithm is then used to reduce memory and CPU time in the paper. To improve the performance of the impedance matrix and ensure fast convergence, a highly effective preconditioning strategy [14] is presented to solve the system of equations without any increase in the computational complexity.

2. GENERALIZED VOLUME-SURFACE INTEGRAL EQUATIONS (GVSIE)

Considering an arbitrary shaped 3-D high contrast inhomogeneous media with permeability $\bar{\bar{\varepsilon}}$ and permittivity $\bar{\bar{\mu}}$, as shown in Figure 1(a). The structure is illuminated by an incident plane wave $(\mathbf{E}^i, \mathbf{H}^i)$ and immersed in a homogeneous medium with permittivity ε_0 and

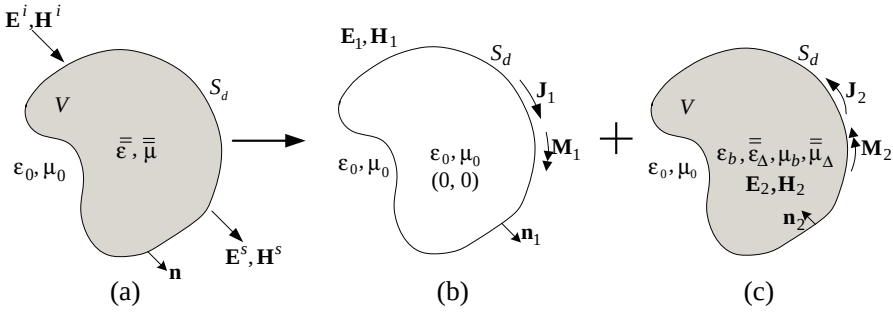

Figure 1. The equivalence principle for the generalized VSIE. (a) Original problem. (b) External equivalence. (c) Internal equivalence.

permeability μ_0. Let S_d denotes the outer surface of the high contrast material, V denotes the volume of the interior space, $\mathbf{n}$ is the outward pointing normal vector on S_d.

According to [6], the domain V can be represented by the constitutive parameters

$$\bar{\bar{\varepsilon}} = \varepsilon_b \bar{\bar{I}} + \bar{\bar{\varepsilon}}_\Delta = \epsilon_b [\bar{\bar{I}} + \varepsilon_b^{-1} \bar{\bar{\varepsilon}}_\Delta] = \varepsilon_b \bar{\bar{\varepsilon}}_\Delta, \tag{1}$$

$$\bar{\bar{\mu}} = \mu_b \bar{\bar{I}} + \bar{\bar{\mu}}_\Delta = \mu_b [\bar{\bar{I}} + \mu_b^{-1} \bar{\bar{\mu}}_\Delta] = \mu_b \bar{\bar{\mu}}_\Delta, \tag{2}$$

where the uniform terms (ϵ_b, μ_b) constitute an equivalent homogeneous background region that can be varied by way of the modulation terms $(\bar{\bar{\varepsilon}}_\Delta, \bar{\bar{\mu}}_\Delta)$. By invoking the equivalence principle, two equivalent problems are formulated, each valid for regions external and internal to the material. In the equivalent problem for the external region, as shown in Figure 1(b), the dielectric surface S_d is replaced by a fictitious surface and the entire region is filled by the homogeneous material of external medium. The field inside the surface S_d is set to zero. The field $(\mathbf{E}_1, \mathbf{H}_1)$ outside the surface S_d can be equivalent to the field produced by the equivalent surface source $(\mathbf{J}_1, \mathbf{M}_1)$ $(\mathbf{J}_1 = \mathbf{J}_s^e, \mathbf{M}_1 = \mathbf{J}_s^m)$ on S_d. Then $(\mathbf{E}_1, \mathbf{H}_1)$ can be expressed as

$$\mathbf{E}_1 = \mathbf{E}^i + Z_1 L_1(\mathbf{J}_s^e) - K_1(\mathbf{J}_s^m), \quad \mathbf{r} \in S_d \tag{3}$$

$$\mathbf{H}_1 = \mathbf{H}^i + \frac{1}{Z_1} L_1(\mathbf{J}_s^m) - K_1(\mathbf{J}_s^e). \quad \mathbf{r} \in S_d \tag{4}$$

The interior equivalent situation is shown in Figure 1(c). In the present situation, in addition to the equivalent surface currents $(\mathbf{J}_2, \mathbf{M}_2)$ on S_d $(\mathbf{J}_2 = -\mathbf{J}_s^e, \mathbf{M}_2 = -\mathbf{J}_s^m)$, we introduce additional the equivalent volumetric currents $\mathbf{J}_v^e$ and $\mathbf{J}_v^m$ in V. Then the electric and magnetic

fields inside the target can be expressed as

$$\mathbf{E}_2 = Z_2 L_2(-\mathbf{J}_s^e) - K_2(-\mathbf{J}_s^m) + \mathbf{E}_2^s(\mathbf{J}_v^e) + \mathbf{E}_2^s(\mathbf{J}_v^m), \quad \mathbf{r} \in V \quad (5)$$

$$\mathbf{H}_2 = \frac{1}{Z_2} L_2(-\mathbf{J}_s^m) + K_2(-\mathbf{J}_s^e) + \mathbf{H}_2^s(\mathbf{J}_v^e) + \mathbf{H}_2^s(\mathbf{J}_v^m). \quad \mathbf{r} \in V \quad (6)$$

By enforcing the continuity of the tangential electric and magnetic fields across each interface, and according to $\mathbf{J}_i = \mathbf{E}_i \times \mathbf{n}_i$, $\mathbf{M}_i = \mathbf{n}_i \times \mathbf{H}_i$ and $\mathbf{n}_1 = -\mathbf{n}_2 = \mathbf{n}$, then combining (3) and (4) with (5) and (6), we can establish the following two new equations,

$$\begin{aligned} &-[Z_1 L_1(\mathbf{J}_s^e) + Z_2 L_2(\mathbf{J}_s^e)] - [K_1(\mathbf{J}_s^m) + K_2(\mathbf{J}_s^m)] + \mathbf{E}_2^s(\mathbf{J}_v^e) + \mathbf{E}_2^s(\mathbf{J}_v^m) \\ &= \mathbf{E}^i, \quad \mathbf{r} \in S_d \end{aligned} \quad (7)$$

$$\begin{aligned} &-[K_1(\mathbf{J}_s^e) + K_2(\mathbf{J}_s^e)] - \left[\frac{1}{Z_1} L_1(\mathbf{J}_s^m) + \frac{1}{Z_2} L_2(\mathbf{J}_s^m)\right] + \mathbf{H}_2^s(\mathbf{J}_v^e) + \mathbf{H}_2^s(\mathbf{J}_v^m) \\ &= \mathbf{H}^i. \quad \mathbf{r} \in S_d \end{aligned} \quad (8)$$

L, K are the operators, given by

$$L_i(X) = -jk_i \int [X + \frac{1}{k_i^2} \nabla(\nabla' \cdot \mathbf{X})] G_i dS', \quad (9)$$

$$K_i(X) = -\int \mathbf{X} \times \nabla G_i dS', \quad (10)$$

where $G_i(\mathbf{r}, \mathbf{r}') = \frac{e^{-jk_i|\mathbf{r}-\mathbf{r}'|}}{4\pi|\mathbf{r}-\mathbf{r}'|}$, $k_i = \omega\sqrt{\mu_i \epsilon_i}$ and $Z_i = \sqrt{\frac{\mu_i}{\varepsilon_i}}$. $i = 1, 2$ refer to the free-space and the background-space, e.g., $k_1 = \omega\sqrt{\mu_0 \epsilon_0}$ and $k_2 = \omega\sqrt{\mu_b \epsilon_b}$. Then Equations (5)–(8) constitute the GVSIE.

To solve the system in (5)–(8) numerically, discretization over the region with material perturbations is carried out using tetrahedral elements. Specifically, based on the PMCHWT and RWG basis function, the boundaries of the homogeneous regions are discretized using the triangular patches. According to the equivalence principle, the equivalent volumetric electric $\mathbf{J}_v^e(\mathbf{r})$ and magnetic currents $\mathbf{J}_v^m(\mathbf{r})$ can be written as

$$\mathbf{J}_v^e(\mathbf{r}) = j\omega \bar{\bar{k}}^e(\mathbf{r}) \cdot \mathbf{D}(\mathbf{r}), \quad (11)$$

$$\mathbf{J}_v^m(\mathbf{r}) = j\omega \bar{\bar{k}}^m(\mathbf{r}) \cdot \mathbf{B}(\mathbf{r}), \quad (12)$$

where $\bar{\bar{k}}^e(\mathbf{r})$ and $\bar{\bar{k}}^m(\mathbf{r})$ stand for the contrast ratio tensor, can be defined as

$$\bar{\bar{k}}^e = \bar{\bar{I}} - \bar{\bar{\varepsilon}}_\Delta^{-1}, \quad (13)$$

$$\bar{\bar{k}}^m = \bar{\bar{I}} - \bar{\bar{\mu}}_\Delta^{-1}. \quad (14)$$

Once the VIE are constructed, the unknown electric flux density $\mathbf{D}(\mathbf{r})$ and magnetic flux density $\mathbf{B}(\mathbf{r})$ can be represented by SWG vector basis functions [1], namely,

$$j\omega\mathbf{D}(\mathbf{r}) = \sum_{n=1}^{Nv} I_{v,n}^{e}\mathbf{f}_{v,n}(\mathbf{r}), \tag{15}$$

$$j\omega\mathbf{B}(\mathbf{r}) = \sum_{n=1}^{Nv} I_{v,n}^{m}\mathbf{f}_{v,n}(\mathbf{r}), \tag{16}$$

in which N_v is the number of faces in V, $I_{v,n}^{e}$ and $I_{v,n}^{m}$ are the unknown expansion coefficients for the volumetric electric and magnetic currents, respectively. $f_{v,n}$ denotes the basis function for the nth face of the tetrahedral cell over the perturbations region V. The surface electric and magnetic currents on S_d can be represented by RWG vector basis functions [2], namely,

$$\mathbf{J}_s^{e}(\mathbf{r}) = \sum_{n=1}^{Nd} I_{s_d,n}^{e}\mathbf{f}_{s,n}(\mathbf{r}), \tag{17}$$

$$\mathbf{J}_s^{m}(\mathbf{r}) = \sum_{n=1}^{Nd} I_{s_d,n}^{m}\mathbf{f}_{s,n}(\mathbf{r}), \tag{18}$$

where N_d is the total number of the common edges on S_d. $I_{s_d,n}^{e}$ and $I_{s_d,n}^{m}$ are the unknown expansion coefficients for the surface electric and magnetic currents on S_d, respectively, and $\mathbf{f}_{s,n}$ represents the nth face basis function for the nth common edge.

Using the extended Galerkin's method and testing the resultant integral equations with a set of testing functions, as a result, the integral equations are converted into a general matrix form. It can be formally written as

$$\begin{bmatrix} Z^{DD} & \eta_0 Z^{DM} & Z^{DD_v} & \eta_0 Z^{DM_v} \\ \eta_0 Z^{MD} & \eta_0^2 Z^{MM} & \eta_0 Z^{MD_v} & \eta_0^2 Z^{MM_v} \\ Z^{D_vD} & \eta_0 Z^{D_vM} & Z^{D_vD_v} & \eta_0 Z^{D_vM_v} \\ \eta_0 Z^{M_vD} & \eta_0^2 Z^{M_vM} & \eta_0 Z^{M_vD_v} & \eta_0^2 Z^{M_vM_v} \end{bmatrix} \begin{bmatrix} I_{s_d}^{E} \\ I_{s_d}^{M}/\eta_0 \\ I_v^{E} \\ I_v^{M}/\eta_0 \end{bmatrix} = \begin{bmatrix} V_{s_d}^{E} \\ \eta_0 V_{s_d}^{H} \\ V_v^{E} \\ \eta_0 V_v^{H} \end{bmatrix} \tag{19}$$

where sub-matrices $Z^{TX}\,(T, X = D, M)$ constitute matrices of traditional PMCHWT, and $Z^{TX}\,(T, X = D_v, M_v)$ constitute matrices of VIE (It should be noted that there VIE is located in homogeneous background medium with permittivity ε_b and permeability μ_b). When the modulation terms are removed, then the GVSIE formulations degenerate into traditional PMCHWT formulations. It should be noted that the wave impedance of free space η_0 is introduced to balance

the magnitude of each operator and make the whole system better conditioned.

3. THE HYBRID EDM-ACA

On the dielectric surface S_d, a RWG element is viewed as a dipole moment model. The nth dipole moment can be obtained by the integration of the surface current, corresponding to edge element n, over the element surface:

$$\mathbf{m}_{s,n}^{t} = \int_{T_n^{\pm}} \mathbf{f}_{s,n} dS' \approx l_{s,n}(\mathbf{r}_{s,n}^{c-} - \mathbf{r}_{s,n}^{c+}). \quad (t = D, M) \tag{20}$$

Similarly, in region V where the material is actually varying, a SWG common face containing two inner adjacent tetrahedrons or a SWG boundary face containing one tetrahedron is viewed as a dipole model. The nth volume electric dipole moment and magnetic dipole moment corresponding to tetrahedrons can be written as

$$\mathbf{m}_{v,n}^{t} = \int_{T_n^{\pm}} \mathbf{f}_{v,n} dV' \approx a_{v,n} \bar{\bar{k}}^{x+}(\mathbf{r}) \cdot \left(\mathbf{r}_{ns}^{c} - \mathbf{r}_{v,n}^{c+}\right) + a_{v,n} \bar{\bar{k}}^{x-}(\mathbf{r}) \cdot \left(\mathbf{r}_{v,n}^{c-} - \mathbf{r}_{ns}^{c}\right), \quad (t = D_v; M_v \text{ and } x = e; m) \tag{21}$$

where $\mathbf{r}_{v,n}^{c\pm}$ and $\mathbf{r}_{ns}^{c}$ are the centroid radius vectors of a pair of tetrahedrons $T_n^{\pm}$ and the nth boundary face associated with T_n^{+}, respectively, and $a_{v,n}$ is the area of the nth common face associated with $T_n^{\pm}$ or the area of the nth boundary face.

Referring to Refs. [7, 8], the radiated electric and magnetic fields of the nth infinitesimal electric dipole at the field point can be expressed as

$$\mathbf{E}_i^t(\mathbf{r}) = \frac{\eta_i}{4\pi}\left[\left(\mathbf{M}_{u,n}^{t} - \mathbf{m}_{u,n}^{t}\right)\left(\frac{jk_i}{R} + C\right) + 2\mathbf{M}_{u,n}^{t} C\right], \quad (t = D; D_v \text{ and } u = s; v) \tag{22}$$

$$\mathbf{H}_i^t(\mathbf{r}) = \frac{jk_i}{4\pi}(\mathbf{m}_{u,n}^{t} \times \mathbf{R})C, \quad (t = D; D_v \text{ and } u = s; v) \tag{23}$$

Similarly, the radiated electric and magnetic fields of the nth infinitesimal magnetic dipole at the field point can be expressed as

$$\mathbf{E}_i^t(\mathbf{r}) = -\frac{jk_i}{4\pi}(\mathbf{m}_{u,n}^{t} \times \mathbf{R})C, \quad (t = M; M_v \text{ and } u = s; v) \tag{24}$$

$$\mathbf{H}_i^t(\mathbf{r}) = \frac{1}{4\pi\eta_i}\left[\left(\mathbf{M}_{u,n}^{t} - \mathbf{m}_{u,n}^{t}\right)\left(\frac{jk_i}{R} + C\right) + 2\mathbf{M}_{u,n}^{t} C\right], \quad (t = M; M_v \text{ and } u = s; v) \tag{25}$$

in which

$$\mathbf{M}_{u,n}^{t} = \frac{(\mathbf{R} \cdot \mathbf{m}_{u,n}^{t})\mathbf{R}}{R^2}, \quad (t = D; D_v, M_v \text{ and } u = s; v) \tag{26}$$

$$C = \frac{1}{R^2}[1 + \frac{1}{jk_iR}], \tag{27}$$

where $\mathbf{R} = \mathbf{r}_{mn} = \mathbf{r}_m - \mathbf{r}_n$, and $R = |\mathbf{R}|$. $\mathbf{r}_m$ and $\mathbf{r}_n$ are the center radius vectors of the nth and the mth equivalent dipole models, respectively.

Then the elements of the impedance matrix are calculated by

$$Z_{mn}^{DT} \approx l_{s,m}[e^{-jk_2R}\mathbf{E}_2^T(R)|_{R=r_m-r_n} \cdot (\mathbf{r}_{s,m}^{c-} - \mathbf{r}_{s,m}^{c+})], \quad (T = D_v, M_v), \quad T_{s,m}^{\pm} \in S_d \tag{28}$$

$$Z_{mn}^{DT} \approx -l_{s,m}\left[\left(e^{-jk_1R}\mathbf{E}_1^T(R) + e^{-jk_2R}\mathbf{E}_2^T(R)\right)\Big|_{R=r_m-r_n} \cdot \left(\mathbf{r}_{s,m}^{c-} - \mathbf{r}_{s,m}^{c+}\right)\right], \quad (T = D, M), \quad T_{s,m}^{\pm} \in S_d \tag{29}$$

$$Z_{mn}^{MT} \approx -l_{s,m}\left[\left(e^{-jk_1R}\mathbf{H}_1^T(R) + e^{-jk_2R}\mathbf{H}_2^T(R)\right)\Big|_{R=r_m-r_n} \cdot \left(\mathbf{r}_{s,m}^{c-} - \mathbf{r}_{s,m}^{c+}\right)\right]. \quad (T = D, M), \quad T_{s,m}^{\pm} \in S_d \tag{30}$$

$$Z_{mn}^{MT} \approx l_{s,m}[e^{-jk_2R}\mathbf{H}_2^T(R)|_{R=r_m-r_n} \cdot (\mathbf{r}_{s,m}^{c-} - \mathbf{r}_{s,m}^{c+})]. \quad (T = D_v, M_v), \quad T_{s,m}^{\pm} \in S_d \tag{31}$$

In (28)–(31), the $l_{s,m}$ is the length of mth common edge associated with a pair of triangle patches $T_{s,m}^{\pm}$ and $\mathbf{r}_{s,m}^{c\pm}$ is the centroid radius vector of $T_{s,m}^{\pm}$.

$$Z_{mn}^{YT} \approx sign(m,n) \begin{cases} a_{v,m}\left[e^{-jk_2R}\Gamma_2^T(R)|_{R=r_m-r_n} \cdot (\mathbf{r}_{v,m}^{c-} - \mathbf{r}_{v,m}^{c+})\right], \\ \qquad\qquad T_m^{\pm} \in V \\ a_{v,m}[e^{-jk_2R}\Gamma_2^T(R)|_{R=r_m-r_n} \cdot (\mathbf{r}_{ms}^{c-} - \mathbf{r}_{v,m}^{c+})], \\ \qquad\qquad T_m^{+} \in V \text{ and } T_m^{-} \notin V \end{cases} \tag{32}$$

where $Y = D_v; M_v$, $T = D, M, D_v, M_v$ and $\Gamma = \mathbf{E}; \mathbf{H}$, and

$$sign(m,n) = \begin{cases} + & \text{elsewhere} \\ - & T_{v,m}^{\pm} \in V \quad \text{and} \quad T_{v,n}^{\pm} \in V \end{cases}. \tag{33}$$

In (32), the $\mathbf{r}_{v,m}^{c\pm}$ and $\mathbf{r}_{ms}^{c}$ are the centroid radius vector of a pair of tetrahedrons $T_{v,m}^{\pm}$ and the mth boundary face, respectively. $a_{v,m}$ is the area of the common face associated with $T_{v,m}^{\pm}$ or the area of the mth boundary face associated with $T_{v,m}^{+}$. Equations (28)–(32) are the exact expressions and valid at arbitrary distances from the dipole. Considering the accuracy and efficiency of the algorithm, the EDM can be applied when the distance between the source and the testing function location is greater than $0.15\lambda_0$ (λ_0 is the wavelength in free space).

As is well known to all that with an increase in size of the object, the elements of the impedance matrix increase quickly and the calculation will cost much memory and CPU time. In this article, the ACA [13] is employed to mitigate this problem. The ACA algorithm is a matrix decomposition algorithm, thus impedance matrix is decomposed into a series of the sub-matrix block with different sizes. The diagonal blocks corresponding to self-group interactions or the interactions of two touching groups are to be computed via the conventional EDM/MoM approach. The numerically rank-deficient matrix blocks corresponding to interactions of well-separated groups will be efficiently compressed through the ACA algorithm. Considering two groups such as group i and group j which are a well-separated group pair and include N_i and N_j dipoles respectively, the interactions Z_{ji} between the two groups can be approximated by the ACA, as

$$\widetilde{Z}_{ji} = U^{N_j \times r} V^{r \times N_i}, \tag{34}$$

where r denotes the effective rank of the submatrix Z_{ji}. Further, $U^{N_j \times r}$ is a matrix of size $N_j \times r$, and $V^{r \times N_i}$ is a matrix of size $r \times N_i$. The more detail of the ACA algorithm can be found in Ref. [13]. The goal of the ACA is to achieve error matrix

$$\|R_{ji}\|_F = \|Z_{ji} - \widetilde{Z}_{ji}\|_F \leq \varepsilon \|Z_{ji}\|_F, \tag{35}$$

where ϵ is a given tolerance, and $\|\cdot\|_F$ represents the matrix Frobenus norm. The accuracy of the ACA can be easily controlled by a given tolerance ε. In the paper, the tolerance $\varepsilon = 10^{-2}$ is used in the ACA algorithm. Clearly, compared with the conventional EDM/MoM, the submatrices are efficiently compressed by the ACA, which reduces the complexity of the memory and the CPU time cost in MVPs from $O(N_i N_j)$ to $O(r(N_i + N_j))$.

Since the elements of impedance matrices $[Z^{TT}(T = D_v, M_v)]$ and $[Z^{TT}(T = D, M)]$ are not in the same order, the EDM/MoM based on the GVSIE formulation results in poorly-conditioned matrices and thus the generalized minimum residual (GMRES) iterative algorithm converges very slowly. In order to improve the performance of the impedance matrix and ensure fast convergence, one effective way is to precondition the coefficient matrix so that the modified system can converge significantly in much less iterations than the original one does. Although we have introduced wave impedance η_0 to balance the magnitude, the elements of impedance matrices $[Z^{TT}(T = D_v, M_v)]$ are still smaller than those of $[Z^{TT}(T = D, M)]$, and then we consider that the basis functions for the dielectric volume are replaced by the new form $\mathbf{f}'_{v,n} = c\mathbf{f}_{v,n}$ (where c is a coefficient to be determined), refer to [14]. Thus, the principal diagonal elements of the new impedance matrix

are nearly in the same order and then the condition number of the preconditioned matrix is significantly decreased compared with that of original one which ensures the faster convergence of the preconditioned matrix.

4. NUMERICAL RESULTS

All the simulations are performed on a personal computer with the Intel(R) Pentium(R) Dual-Core CPU E2200 with 2.0 GHz (only one core was used) and 2.0 GB RAM. The GMRES iterative solver is employed to obtain an identical residual error 0.001.

First, we consider the scattering problem of a high contrast two-layer concentric sphere with inner radius $r_2 = 0.1\lambda$, outer radius $r_1 = 0.5\lambda$, $\varepsilon_{r2} = 20$ and $\varepsilon_{r1} = 10$. The bistatic radar cross sections (RCS) results are obtained for a plane wave at normal incidence with $\theta = 0^\circ$, $\phi = 0^\circ$. According to the factorization, we chose $\varepsilon_b = 10$ with in the regions where $\varepsilon_\Delta = 2$. Then the VIE in (5) and (6) are only invoked inside the smaller embedded sphere instead of the entire scattering domain and the PMCHWT is only applied on the surface of the larger sphere. In order to ensure the accuracy of the result, the smaller embedded sphere is discretized into tetrahedrons by $\lambda/20$ average edge length, and then only 1236 unknowns are produced, the larger sphere is discretized by triangle elements $\lambda/12$, and then 1986 unknowns are produced. It should be remarked here that the magnetic surface current unknowns could be in consistent with the electric surface current unknowns, as a result, the total unknowns are 5208. By

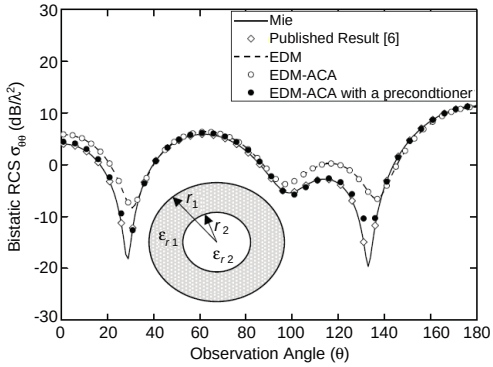

Figure 2. Bistatic RCS of a two-layer sphere with inner radius $r_2 = 0.1\lambda$, outer radius $r_1 = 0.5\lambda$, $\varepsilon_{r2} = 20$ and $\varepsilon_{r1} = 10$ excited by a plane wave with the incident direction of $(\theta, \phi) = (0^\circ, 0^\circ)$.

comparison, if the usual VIE was used throughout the entire dielectric domain, it would require approximately 300000 unknowns. Obviously, the GVSIE method can reduce the total number of unknowns greatly compared with the conventional VIE method. In the ACA algorithm, all the unknowns are divided into 36 nonempty groups and the size of each group is 0.2λ.

Figure 2 gives the bistatic RCS for $\theta\theta$ polarization calculated by the Mie, EDM, EDM-ACA and EDM-ACA with a preconditioner (multiplying c ($c = 174547$)). The results have been compared with that from [6]. The memory needs 263 MB when only EDM is used, and the convergence number is 580, then it cost 2570 s. After employing ACA algorithm, the convergence number is unchanged, but the memory requirements are reduced to 209 MB, then 1295 s are needed. However, the results of EDM and EDM-ACA methods have some errors when compared with those of the Mie solution and [6] because of the ill-conditioned impedance matrix. The accuracy has been greatly improved after multiplying c ($c = 174547$)), and the memory requirements and time are further reduced to 200 and 1039 s, respectively. The result calculated by the EDM-ACA method after preconditioning is in excellent agreement with those of the Mie solution and [6]. So, all the results of the next example are calculated by EDM-ACA after preconditioning.

We next consider a hemisphere radome being illuminated by a plane wave propagating along the z direction at the frequency of 0.15 GHz. The inner and outer diameters of the radome are 0.8 m and 1.0 m, respectively, and $\varepsilon_r = 4$. The radome is discretized into 3538 tetrahedrons and 1296 triangle cells by $\lambda_g/10$ average edge length,

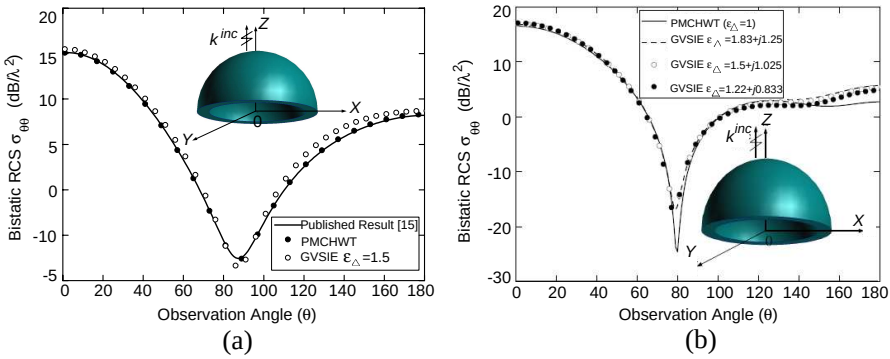

Figure 3. Bistatic RCS of hemisphere radome. (a) Radome considered in [15]. (b) High contrast radome.

and then 7724 volumetric unknowns and 1944 surface unknowns are produced, thus resulting in total 11612 unknowns. If VIE is used for the problem, 30126 unknowns are needed. It can be seen from Figure 3(a) that with the selected ε_Δ, our formulation compares well with [15] and the PMCHWT method ($\varepsilon_\Delta = 1$). To further demonstrate the robustness of our method, a higher contrast material is presented in Figure 3(b) where the permittivity of the radome is increased to $\varepsilon_r = 17.97 - j14.57$. The radome will be modeled using different background medium and different variation, so as to represent a material having an ε_r. All of the chosen backgrounds medium are lossy to ensure fast convergence (if the backgrounds medium are not lossy, they can not converge in 1000 steps). The discretization density is same to that of $\varepsilon_r = 4$. All results are calculated by EDM-ACA after multiplying c ($c = 1000$). The results compare well with each other, as are shown in Figure 3(b). The curves slightly shifted away from that calculated by PMCHWT with the increase of ε_Δ. It is due to the mesh error, that is to say the larger ε_Δ is, then the more meshes are needed. It is important to further note that although the contrast of the radome was increased, and different background medium are chosen, the same discretization density was used for all of them. The presented results suggest that there has some sense in which the GVSIE is applied in the analysis of scattering from high-contrast material.

5. CONCLUSIONS

The GVSIE formulation is used for the calculation of electromagnetic scattering from high contrast materials. The advantage of the GVSIE is that the VIE is only invoked within region where the material is actually varying, and PMCHWT is employed at the boundaries of the volume region where Green's functions for the high contrast background medium are used. The GVSIE solved by the MoM using SWG and RWG basis functions leads to fewer unknowns making it useful in computing scattering applications of arbitrary shaped high contrast media. Further, the EDM-ACA method combined with a preconditioner is implemented to reduce memory requirements, CPU time and improve accuracy for solving the electromagnetic scattering problems.

ACKNOWLEDGMENT

The work is supported by the National Natural Science Foundation of China under Grant No. 61071019, the Joint Funding projects of the Aerospace Science Foundation Office of China No. 2008ZA52006.

REFERENCES

1. Schaubert, D. H., D. R. Wilton, and A. W. Glisson, "A tetrahedral modeling method for electromagnetic scattering by arbitrarily shaped inhomogeneous dielectric bodies," *IEEE Trans. Antennas Propag.*, Vol. 32, 77–85, 1984.
2. Rao, S. M., D. R. Wilton, and A. W. Glisson, "Electromagnetic scattering by surfaces of arbitrary shape," *IEEE Trans. Antennas Propag.*, Vol. 30, No. 3, 409–418, 1982.
3. Poggio, A. J. and E. K. Miller, *Integral Equation Solution of Three Dimensional Scattering Problems,* Chapter 4, Elmsford, Permagon, NY, 1973.
4. Chang, Y. and R. F. Harrington, "A surface formulation for characteristic modes of material bodies," *IEEE Trans. Antennas Propag.*, Vol. 25, 789–795, 1977.
5. Wu, T. K. and L. L. Tsai, "Scattering from arbitrarily-shaped lossy dielectric bodies of revolution," *Radio Sci.*, Vol. 12, 709–718, 1977.
6. Usner, B. C., K. Sertel, M. A. Carr, and J. L. Volakis, "Generalized volume-surface integral equation for modeling inhomogeneities within high contrast composite structures," *IEEE Trans. Antennas Propag.*, Vol. 54, No. 1, 68–75, 2006.
7. Yuan, J. D., C. Q. Gu, and G. D. Han, "Efficient generation of method of moments matrices using equivalent dipole-moment method," *IEEE Antennas and Wireless Propag. Lett.*, Vol. 8, 716–719, 2009.
8. Deng, X. Q., C. Q. Gu, and Y. G. Zhou, "Electromagnetic scattering by arbitrary shaped three-dimensional conducting objects covered with electromagnetic anisotropic materials," *ACES Journal*, Vol. 26, No. 11, 886–892, 2011.
9. Gurel, L., T. Malas, and L. Gurel, "Solutions of large scale electromagnetics problems using an iterative inner-outer scheme with ordinary and approximate multilevel fast multipole algorithms," *Progress In Electromagnetics Research*, Vol. 106, 203–223, 2010.
10. Wang, C. F., L. W. Li, P. S. Kooi, and M. S. Leong, "Efficient capacitance computation for three dimensional structures based on adaptive integral method," *Progress In Electromagnetics Research*, Vol. 30, 33–46, 2011.
11. Chen, X. L., Z. Y. Niu, Z. Li, and C. Q. Gu, "A hybrid fast dipole method and adaptive modified characteristic basis function method for electromagnetic scattering from perfect

electric conduction targets," *Journal of Electromagnetic Waves and Applications*, Vol. 25, Nos. 14–15, 1940–1952, 2011.

12. Chen, X. L., Z. Li, Z. Y. Niu, and C. Q. Gu, "Analysis of electromagnetic scattering from PEC targets using improved fast dipole method," *Journal of Electromagnetic Waves and Applications*, Vol. 25, No. 16, 2254–2263, 2011.
13. Zhao, K., M. N. Vouvakis, and J.-F. Lee, "The adaptive cross approximation algorithm for accelerated method of moments computations of EMC," *IEEE Trans. Electromagn. Compat.*, Vol. 47, No. 4, 763–773, 2005.
14. Guo, J. L., J. Y. Li, and Q. Z. Liu, "Electromagnetic analysis of coupled conducting and dielectric targets using MoM with a preconditioner," *Journal of Electromagnetic Waves and Applications*, Vol. 19, No. 9, 1223–1236, 2005.
15. Li, X. M., C. M. Tong, S. H. Fu, and J. J. Li, "A study on EM scattering characteristics of radome," *Modern Radar*, Vol. 31, No. 10, 95–97, 2009.